Pressure Effects

DOI: 10.1002/ange.200705819

[Mn_6] under Pressure: A Combined Crystallographic and Magnetic Study**

Alessandro Prescimone, Constantinos J. Milios, Stephen Moggach, John E. Warren, Alistair R. Lennie, Javier Sanchez-Benitez, Konstantin Kamenev, Roland Bircher, Mark Murrie, Simon Parsons, and Euan K. Brechin**

While investigating the coordination chemistry of derivatized salicylaldoximes (R-saoH_2) in the synthesis of Mn_6 single-molecule magnets (SMMs) we found that the exchange between the metal centers was weak and typically only a few wavenumbers (<1–$2\ cm^{-1}$) in magnitude.[1] Structurally distorting the molecule "internally" by deliberate chemical modification of the magnetic core (the twisting of the Mn-N-O-Mn moiety) allowed us to switch the exchange from antiferromagnetic to ferromagnetic, thus producing SMMs with ground states of $S=12$ and greatly enhanced blocking temperatures.[2] An alternative method of achieving such a switch is to exert "external" hydrostatic pressure.[3] This is an attractive proposition since it offers the potential to provide detailed information about the relationship between structure and magnetic properties, especially if the magnetic studies can be coupled with high-pressure crystallography. To date the only SMMs to have been studied under pressure are the prototype [Mn_{12}OAc] molecule and the cubane [$Mn_4O_3Br(OAc)_3(dbm)_3$] (Hdbm = dibenzoylmethane); these compounds were studied by a combination of high-pressure SQUID magnetometry and high-pressure inelastic neutron scattering (INS).[4–7] The fundamental problems associated with high-pressure (HP) measurements on complex molecular systems originate from a simple lack of technology—the availability of the appropriate pressure cells to be able to perform experiments at the elevated pressures (and low temperatures) at which structural (and magnetic) change occurs. Indeed, although the above studies revealed changes in the magnetic response, their explanation is hindered by the lack of high-pressure crystallographic data, and so remain somewhat speculative. Herein we present our initial study of the combined HP crystallography and HP magnetism of the single-molecule magnet [$Mn^{III}_6O_2$(Et-sao)$_6$(O_2CPh(Me)$_2$)$_2$(EtOH)$_6$] (**1**; Et-saoH$_2$ = 2-hydroxyphenylpropanone oxime).[2]

Complex **1** crystallizes in the monoclinic space group $P2_1/n$ with the molecule lying on an inversion center and can be described (Figure 1) as consisting of two parallel off-set, stacked {$Mn^{III}_3(\mu_3\text{-O})$}$^{7+}$ triangular subunits linked through two "central" oximate O atoms and two "peripheral" phenoxide O atoms to give a {$Mn^{III}_6(\mu_3\text{-O})_2(\mu_3\text{-ONR})_2(\mu\text{-ONR})_4$}$^{8+}$ core. The bridging between neighboring Mn ions within each triangle occurs through an NO oximate group, such that each Mn_2 pair forms an -Mn-N-O-Mn- moiety, and thus the Mn_3 triangle forms an (-Mn-O-N)$_3$ ring. The coordination spheres of the Mn ions are completed by two terminal carboxylate groups (one on each triangle), a phenoxide O atom, and terminal alcohol molecules. All Mn ions are in the 3+ oxidation state, as confirmed by a combination of bond-length considerations, bond-valence sum (BVS) calculations, and

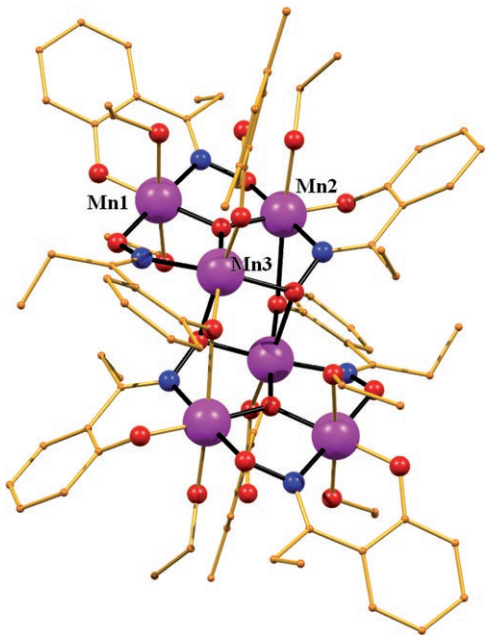

Figure 1. The molecular structure of complex **1**. Color code: Mn purple, O red, N blue, C gold.

[*] A. Prescimone, Dr. C. J. Milios, S. Moggach, Dr. J. Sanchez-Benitez, Dr. K. Kamenev, Prof. S. Parsons, Dr. E. K. Brechin
Schools of Chemistry and Engineering and Centre for Science at Extreme Conditions (CSEC), The University of Edinburgh
West Mains Road, Edinburgh, EH9 3JJ (UK)
Fax: (+44) 131-650-6453
E-mail: ebrechin@staffmail.ed.ac.uk
s.parsons@ed.ac.uk
Dr. M. Murrie
Department of Chemistry, The University of Glasgow
University Avenue, Glasgow G12 8QQ (UK)
Dr. J. E. Warren, Dr. A. R. Lennie
Daresbury Laboratory, Warrington, Chesire, WA4 4AD (UK)
Dr. R. Bircher
Bragg Institute, Building 87
The Australian Nuclear Science and Technology Organisation
PMB 1, Menai NSW 2234 (Australia)

[**] We thank the EPSRC for funding.

charge balance.[2] All are six-coordinate, adopting distorted octahedral geometry with their Jahn–Teller (JT) axes approximately coparallel and perpendicular to the $\{Mn_3O\}^{7+}$ planes.

Previous magnetic studies have shown that complex **1** is characterized by a ground state of $S = 12$, which can be rationalized by assuming ferromagnetic interactions between the six Mn^{3+} ions; the origin of the ferromagnetic exchange is the severe twisting of the Mn-N-O-Mn moieties (the three torsion angles are all above an angle of ca. 31°).[2]

High-pressure crystallographic experiments were carried out by using a Merrill–Bassett diamond anvil cell with a half-opening angle of 40° and equipped with Boehler-Almax-cut diamonds with 600 micron culets and a tungsten gasket.[8] Petroleum ether was used as the hydrostatic medium. A small ruby chip was also loaded into the cell as the pressure calibrant: the ruby fluorescence was used to measure the pressure. The application of hydrostatic pressure up to 15 kbar causes significant structural change: a) the Mn-N-O-Mn torsion angles become flatter (less twisted); b) the JT bond lengths are altered; and c) the intermolecular interactions are shortened. The changes are summarized in Figure 2 and Tables 1 and 2. The Mn-N-O-Mn torsion angles change rather dramatically: that between Mn1 and Mn3 changes from 34.8° to 28°; that between Mn2 and Mn3 changes from 39.1° to 34°; and that between Mn1 and Mn2 changes from 42.9° to 44°. Significantly the torsion angle between Mn1 and Mn3 (and symmetry equivalent) falls below the value previously reported as being responsible for the switch in the pairwise exchange interaction between the two metals from ferromagnetic to antiferromagnetic.[2]

The Jahn–Teller axes show two different responses (Table 2). We observe a continuous compression for Mn1 and Mn2: 2.132, 2.434 Å to 2.110, 2.365 Å for the former and 2.196, 2.480 Å to 2.152, 2.401 Å for the latter. The behavior of Mn3 is rather peculiar. The JT axis first elongates up to 5 kbar and then continually compresses as the pressure is increased to 15 kbar. The overall change equates to a small increase in the Mn3–O14 distance from 2.242(3) to 2.263(13) Å and a small decrease in the Mn3–O124 distance, from 2.333 to 2.316 Å.

The pressure-induced contraction of the unit cell is summarized in Table 3 and can be attributed to the reduction of the voids present in the lattice. The effect on the packing of the molecules in the crystal structure is to reduce the intermolecular separation; however, this effect does not induce any significant intermolecular hydrogen bonding or π–π stacking. The coordinated ethanol molecules create a number of intramolecular hydrogen bonds: between the H atoms belonging to the alcohols and the noncoordinated oxygen atom of the carboxylate groups and the monodentate oximic oxygen atoms. The torsion angle between Mn1 and Mn2 is the one least affected by pressure, presumably because of the increased flexibility of Mn3, which resides at the periphery of the cluster. However, this effect may also be due, at least in part, to the hydrogen bonding between the alcohols coordinated to Mn3 (and symmetry equivalents) and the phenolic O atom from the ligand bridging Mn1 and Mn3 as well as the close contact to the H atom from the oximic O atom of the ligand between Mn1 and Mn2.

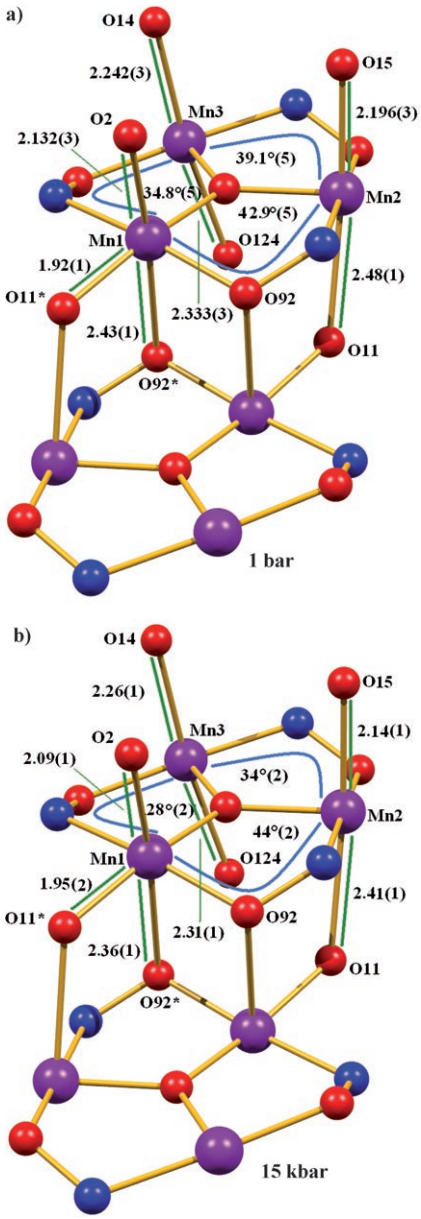

Figure 2. Magnetic cores of **1** at a) 1 bar and b) 15 kbar; distances in Å and torsion angles in °.

Table 1: Comparison of the amplitude of the Mn-O-N-Mn torsion angles [°] for **1** as a function of pressure.

P [kbar]	Mn1-O-N-Mn2	Mn2-O-N-Mn3	Mn3-O-N-Mn1
0	42.9° (5)	39.1° (5)	34.8° (5)
5	43.3° (13)	37.2° (13)	31.8° (14)
10	43.6° (16)	34.6° (17)	29.0° (18)
15	44° (2)	34° (2)	28° (2)

For the high-pressure magnetic measurements a cell of piston-cylinder design capable of reaching 20 kbar was constructed. The body of the pressure cell was made of nonmagnetic CrNiAl and BERYLCO-25 alloys with zirconia rods used as pistons.[9] The sample was contained inside a polytetrafluoroethylene (PTFE) capsule, and Daphne 7373 oil (IDEMITSU-ILS) was used as the pressure transmitting medium. Pressure was applied in a hydraulic press and was

Table 2: Comparison of the bond lengths [Å] of the Jahn–Teller axes for **1** as a function of pressure.

P [kbar]	Mn1–O2	Mn1–O92*	Mn2–O15
0	2.132(3)	2.434(3)	2.196(3)
5	2.134(6)	2.404(6)	2.175(7)
10	2.117(7)	2.364(7)	2.154(9)
15	2.110(8)	2.365(10)	2.152(12)
P [kbar]	Mn2–O11	Mn3–O14	Mn3–O124
0	2.480(3)	2.242(3)	2.333(3)
5	2.457(8)	2.281(7)	2.343(8)
10	2.438(8)	2.267(9)	2.317(10)
15	2.401(12)	2.263(13)	2.316(13)

Table 3: Comparison of the lengths of the axes and the volume of the unit cell for **1** as a function of pressure.

P [kbar]	*a* [Å]	*b* [Å]	*c* [Å]	*V* [Å^3]
0	12.9120(2)	23.5530(4)	15.1900(3)	4404.53(14)
5	12.7241(13)	23.184(7)	14.962(2)	4196.8(14)
10	12.5241(8)	22.836(3)	14.6696(10)	3987.9(7)
15	12.4723(13)	22.703(5)	14.5813(15)	3922.6(10)

calibrated by the load. The highest pressure employed was 17.5 kbar.

Under ambient conditions complex **1** displays an increase in the value of the $\chi_M T$ product with decreasing temperature, and the data are well simulated by the Hamiltonian in Equation (1) to afford the parameters $g = 2.00$ and $J = 1.75\ \mathrm{cm}^{-1}$.[2]

$$\hat{H} = -2J(\hat{S}_1 \cdot \hat{S}_2 + \hat{S}_2 \cdot \hat{S}_3 + \hat{S}_1 \cdot \hat{S}_3 + \hat{S}_{1'} \cdot \hat{S}_{2'} + \hat{S}_{2'} \cdot \hat{S}_{3'} + \hat{S}_{1'} \cdot \hat{S}_{3'} + \hat{S}_1 \cdot \hat{S}_{2'} + \hat{S}_1 \cdot \hat{S}_{1'} + \hat{S}_2 \cdot \hat{S}_{1'}) \quad (1)$$

The equivalent high-pressure $\chi_M T$ versus T plots are shown in Figure 3 and show a constant pressure-dependent variation (decrease) in the height of the low-temperature peak and in the slope of the curve. This result clearly suggests a decrease in the magnitude of $|J|$ or a change (ferromagnetic→antiferromagnetic) in one or more of the pairwise exchange interactions. The problems associated with the large background contribution of the cell (at high temperatures) do not permit rigorous quantitative analysis of the data, so what follows should be treated as a qualitative analysis of the observed trends. For each pressure we attempted to simulate the susceptibility data to obtain values of S and J. For the data at 17.5 kbar it is impossible to reproduce the curve employing only one J value [Eq. (1)]. This result is consistent with the crystallographic data; the presence of one (Mn1-N-O-Mn3) torsion angle below 31° suggests an antiferromagnetic exchange between these two metals.[2] Indeed the data can be satisfactorily modeled by employing a Hamiltonian with two J values [Eq. (2) and Figure 4] to afford the parameters $g = 2.00$ and $J_1 = 1.33\ \mathrm{cm}^{-1}$ and $J_2 = -0.45\ \mathrm{cm}^{-1}$.

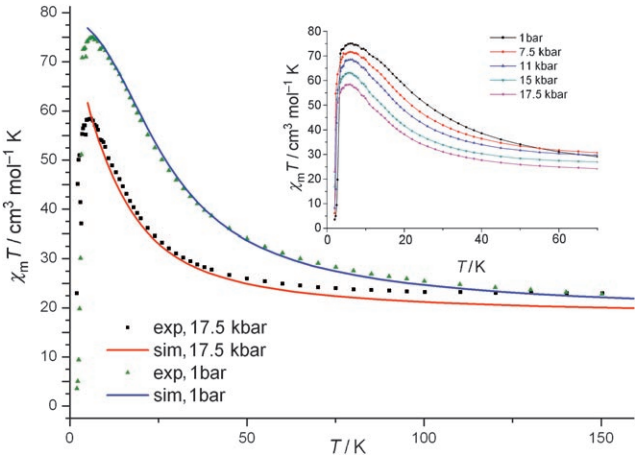

Figure 3. Plots of $\chi_M T$ versus T for **1** recorded in the temperature range 150–5 K and 60–5 K (inset) shown at the indicated pressures. The solid lines represent simulations of the data; see text for details.

$$\hat{H} = -2J_1(\hat{S}_1 \cdot \hat{S}_2 + \hat{S}_2 \cdot \hat{S}_3 + \hat{S}_{1'} \cdot \hat{S}_{2'} + \hat{S}_{2'} \cdot \hat{S}_{3'} + \hat{S}_1 \cdot \hat{S}_{1'} + \hat{S}_1 \cdot \hat{S}_{2'} + \hat{S}_2 \cdot \hat{S}_{1'}) - 2J_2(\hat{S}_1 \cdot \hat{S}_3 + \hat{S}_{1'} \cdot \hat{S}_{3'}) \quad (2)$$

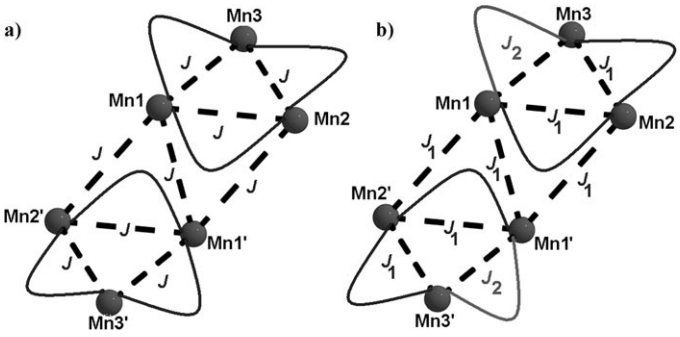

Figure 4. Interactions used to simulate the $\chi_M T$ versus T data for **1** with a 1J model (a) and a 2J model (b).

The simulations suggest the ground state is still $S = 12$ but with the $S = 11$ and $S = 10$ excited states now much closer in energy. Under ambient conditions, the first excited state ($S = 11$) was 8.3 cm^{-1} and the second ($S = 10$) was 16.8 cm^{-1} higher in energy. At the highest pressure measured, the equivalent energy gaps are 1.5 cm^{-1} and 2.98 cm^{-1}, respectively. The simulations of the lower pressure data (Figure 3, Table 4) accordingly show a near linear decrease in the magnitude of $|J|$ with increasing pressure: at 7.5 kbar, $J = 1.45\ \mathrm{cm}^{-1}$; at 11 kbar, $J = 1.20\ \mathrm{cm}^{-1}$ employing Equation (1). At 15 kbar the 1J model cannot successfully simulate the data, and we need to employ Equation (2), which affords $g = 2.00$, $J_1 = 1.35\ \mathrm{cm}^{-1}$, and $J_2 = -0.10\ \mathrm{cm}^{-1}$ and the first ($S = 11$) and second excited states ($S = 10$) are 2.9 cm^{-1} and 5.8 cm^{-1} higher than the ground state ($S = 12$).

Table 4: Comparison of the J values and the energy differences between the spin states for **1** as a function of pressure.

P [kbar]	*S*	*J* [cm^{-1}]	E_1 [cm^{-1}] (S_1)	E_2 (S_2)
0	12	1.75	8.3 ($S = 11$)	16.8 ($S = 10$)
7.5	12	1.45	6.9 ($S = 11$)	14.5 ($S = 10$)
11	12	1.20	5.7 ($S = 11$)	11.5 ($S = 10$)
15	12	1.35, −0.10	2.9 ($S = 11$)	5.8 ($S = 10$)
17.5	12	1.33, −0.45	1.5 ($S = 11$)	2.98 ($S = 10$)

Under ambient conditions, the decrease of $|J|$ and the concomitant decrease in the energy gap between the ground and excited states, which can be thought of as an increased nesting of the excited-state multiplets on the ground state, manifests itself in the decrease of the effective energy barrier for magnetization reversal, and the appearance of hysteresis loops at lower temperatures or with smaller coercive fields.[1,2] In reality, the (ambient-pressure) spin dynamics of these Mn_6 molecules is very complicated. Indeed the "giant-spin" picture is completely inadequate to describe their behavior properly since excited-state S multiplets play a key role in determining the effective energy barrier for the magnetization reversal (we observe tunneling processes involving pairs of states with different total spin).[10] This picture also appears to be true for the (same) molecule under pressure. The trend observed in the high-pressure hysteresis loops (Figure 5) clearly shows a decrease in coercivity with

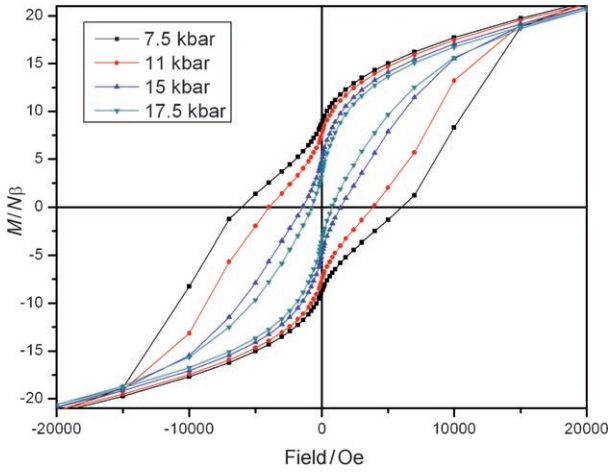

Figure 5. Magnetic hysteresis of **1** at 2 K and the indicated pressures.

increased pressure, which is consistent with a decrease in $|J|$, and an increase in S mixing (or a decrease in $|D|$), although the complicated nature of these molecules requires high-pressure INS and high-pressure EPR measurements for full clarification. These studies are in progress and will be reported in a full paper along with a detailed analysis of ac susceptibility measurements, which will require some modifications in the design of the SQUID pressure cell. These studies will also help to elucidate the effect on $|D|$ of the change in Jahn–Teller bond lengths, and whether JT isomerism (as seen in Mn_{12})[4–7] is also a contributing factor. In addition, a new steel-free crystallographic pressure cell will allow us to repeat the crystallography down to liquid nitrogen temperatures.

In conclusion, an initial series of high-pressure crystallographic measurements on the Mn_6 SMM reveal significant changes in the intramolecular geometry of the magnetic core of the molecule, demonstrating that huge structural changes can occur upon applied external pressure. These topological changes have a knock-on effect upon the magnetic properties of the molecule: the flattening of the Mn-N-O-Mn torsion angles decreases the magnitude of the ferromagnetic exchange between the metals and, in one case, switches the exchange from ferro- to antiferromagnetic. The change in the JT bond lengths are significant and may influence the value of $|D|$. The combined result is a decrease in the energy gap between the ground and excited states, an increased nesting of the excited-state multiplets, and a decrease in the effective energy barrier for magnetization reversal.

Experimental Section

1 was made as described previously.[2]

High-pressure crystallography experiments were carried out on a Bruker APEX-II diffractometer at Station 9.8 at the SRS facility in Daresbury with a wavelength $\lambda = 0.4865$ Å at room temperature. A Merrill–Bassett Be-free diamond anvil cell was used.[8] CCDC 671313, 671314, and 671315 contain the supplementary crystallographic data for this paper. These data can be obtained free of charge from The Cambridge Crystallographic Data Centre via www.ccdc.cam.ac.uk/data_request/cif. Magnetization measurements at ambient and high pressure were carried out in a Magnetic Property Measurement System (Quantum Design, USA) magnetometer equipped with a 5-T magnet operating in the temperature range 300–2 K.

Received: December 19, 2007
Published online: March 5, 2008

Keywords: high-pressure chemistry · magnetic properties · manganese · single-molecule magnets · solid-state structures

[1] a) C. J. Milios, A. Vinslava, P. A. Wood, S. Parsons, W. Wernsdorfer, G. Christou, S. P. Perlepes, E. K. Brechin, *J. Am. Chem. Soc.* **2007**, *129*, 8–9; b) C. J. Milios, A. Vinslava, W. Wernsdorfer, A. Prescimone, P. A. Wood, S. Parsons, S. P. Perlepes, G. Christou, E. K. Brechin, *J. Am. Chem. Soc.* **2007**, *129*, 6547–6561.

[2] a) C. J. Milios, A. Vinslava, S. Moggach, S. Parsons, W. Wernsdorfer, G. Christou, S. P. Perlepes, E. K. Brechin, *J. Am. Chem. Soc.* **2007**, *129*, 2754–2755; b) C. J. Milios, R. Inglis, R. Bagai, W. Wernsdorfer, A. Collins, S. Moggach, S. Parsons, S. P. Perlepes, G. Christou, E. K. Brechin, *Chem. Commun.* **2007**, 3476–3478; c) C. J. Milios, R. Inglis, A. Vinslava, R. Bagai, W. Wernsdorfer, S. Parsons, S. P. Perlepes, G. Christou, E. K. Brechin, *J. Am. Chem. Soc.* **2007**, *129*, 12505–12511.

[3] R. Bircher, G. Chaboussant, C. Dobe, H. U. Güdel, S. T. Ochsenbein, A. Sieber, O. Waldmann, *Adv. Funct. Mater.* **2006**, *16*, 209–220, and references therein.

[4] A. Sieber, R. Bircher, O. Waldmann, G. Carver, G. Chaboussant, H. Mutka, H. U. Güdel, *Angew. Chem.* **2005**, *117*, 4311–4314; *Angew. Chem. Int. Ed.* **2005**, *44*, 4239–4242.

[5] A. Sieber, G. Chaboussant, R. Bircher, C. Boskovic, H. U. Güdel, G. Christou, *Phys. Rev. B* **2004**, *70*, 172413.

[6] Y. Suzuki, K. Takeda, K. Awaga, *Phys. Rev. B* **2003**, *67*, 132402.

[7] K. Awaga, Y. Suzuki, H. Hachisuka, K. Takeda, *J. Mater. Chem.* **2006**, *16*, 2516–2521.

[8] L. Merrill, W. A. Bassett, *Rev. Sci. Instrum.* **1974**, *45*, 290.

[9] J. Sanchez-Benitez, K. Kamenev, unpublished results.

[10] S. Carretta, T. Guidi, P. Santini, G. Amoretti, O. Pieper, B. Lake, J. van Slageren, W. Wernsdorfer, H. Mutka, M. Russina, C. J. Milios, E. K. Brechin, *Phys. Rev. Lett.* **2007**, submitted.

